Tikrit Journal of Engineering Sciences (2025); 32(2): 1937
DOI: http://doi.org/10.25130/tjes.32.2.13

IRAQI Academic Scientific Journals

ISSN: 1813-162X (Print); 2312-7589 (Online)

Tikrit Journal of Engineering Sciences

available online at: http://www.tj-es.com

TJES Tikrit Journal of Engineering Sciences

Assessment of the Riverbank Stability for Tigris River in Salahaddin Governorate/Iraq Using BSTEM Model

Mohammed F. Yass *[a], **Rasul M. Khalaf** [b]

[a] Civil Engineering Department, College of Engineering, Tikrit University, Tikrit, Iraq.
[b] Water Recourses Department, College of Engineering, University of Al Mustansiriyah, Baghdad, Iraq.

Keywords:
Riverbank Stability; Tigris River; Safety Factor; BSTEM; HEC-RAS.

Highlights:

- *BSTEM-HEC-RAS model assessed Tigris Riverbank stability under flow variations (420–1100 m³/s).*
- *Safety factor (SF) analysis revealed conditional stability in Baiji and Tikrit (SF 1.2–1.3).*
- *Higher flows increased stability due to confining pressure, while lower flows raised erosion risks.*

ARTICLE INFO

Article history:

Received	23 Dec.	2023
Received in revised form	14 Mar.	2024
Accepted	16 Apr.	2024
Final Proofreading	07 Mar.	2025
Available online	26 May	2025

Citation: Yass MF, Khalaf RM. **Assessment of the Riverbank Stability for Tigris River in Salahaddin Governorate/Iraq Using BSTEM Model**. *Tikrit Journal of Engineering Sciences* 2025; **32**(2): 1937.
http://doi.org/10.25130/tjes.32.2.13

Corresponding author:

Mohammed F. Yass

Civil Engineering Department, College of Engineering, Tikrit University, Tikrit, Iraq.

Abstract: The riverbanks are a critical component of river ecosystems that provide various ecological, social, and economic benefits. Effective riverbank management is essential for maintaining its functions while minimizing the risks associated with instability. The fluctuation of water levels in the river negatively affects riverbank stability; therefore, the present study aims to examine the instability of the riverbank caused by the variations in water flow within the Tigris River as the basis of analysis. The flow variation effects during (2022) in Salah Al-Din Governorate, which began from the Makhoul dam site (upstream) to the end of Tikrit City (downstream), were investigated by computing a series of safety factors related to outflow events for (20) cross sections along the (82) km reach of Tigris River. The BSTEM algorithm integrated into the HEC-RAS model package was utilized. The results showed that the rate of change in flow at each cross-section impacts the calculated safety factor. Also, the results showed that all cross-sections were stable, and some were conditional stable, meaning that the riverbank is not entirely stable, however, still holding up under the existing conditions. However, caution should be exercised, and it may require monitoring and evaluation to prevent future instability issues.

تقييم استقرار الضفاف النهرية لنهر دجلة في محافظة صلاح الدين/العراق باستخدام نموذج BSTEM

محمد فائق ياس [1]، رسول مجبل خلف [2]

[1] قسم الهندسة المدنية / كلية الهندسة / جامعة تكريت / تكريت – العراق.

[2] قسم هندسة الموارد المائية / كلية الهندسة / الجامعة المستنصرية / بغداد – العراق.

الخلاصة

تُعتبر الضفاف النهرية عنصرًا حيويًا في النظم البيئية النهرية، حيث توفر مجموعة من الفوائد البيئية والاجتماعية والاقتصادية. وتعد الإدارة الفعالة للضفاف ضرورية للحفاظ على وظائفها مع الحد من المخاطر المرتبطة بعدم استقرارها. تؤثر التقلبات في منسوب مياه النهر سلبًا على استقرار الضفاف؛ لذا تهدف هذه الدراسة إلى تحليل عدم استقرار الضفاف الناتج عن التغيرات في التدفق المائي لنهر دجلة كأساس للبحث. تم تقييم تأثيرات التباين في التدفق خلال عام (٢٠٢٢) في محافظة صلاح الدين، بدءًا من موقع سد مكحول (منبعًا) وحتى نهاية مدينة تكريت (مصبًا)، عبر حساب سلسلة من عوامل الأمان المرتبطة بأحداث التدفق لـ(٢٠) مقطعًا عرضيًا على امتداد (٨٢) كيلومترًا من النهر. وتم استخدام خوارزمية BSTEMالمدمجة في حزمة نموذج HEC-RAS. أظهرت النتائج أن معدل التغير في التدفق عند كل مقطع عرضي يؤثر على عامل الأمان المحسوب. كما بينت النتائج أن جميع المقاطع كانت مستقرة، وبعضها كان مستقراً بشروط، مما يشير إلى أن الضفة ليست مستقرة تمامًا، لكنها تحافظ على تماسكها تحت الظروف الحالية. ومع ذلك، يُوصى بتوخي الحذر واعتماد آليات مراقبة وتقييم دورية لمنع حدوث مشاكل عدم الاستقرار في المستقبل.

الكلمات الدالة: استقرار ضفة النهر؛ نهر دجلة؛ عامل الأمان؛ BSTEM؛ HEC-RAS.

1.INTRODUCTION

Human societies have recognized the indispensable role of water in shaping their existence. Rivers and their tributaries have acted as nurturing cradles for civilizations across time, for instance, the mesmerizing tapestry of Mesopotamia, the ancient realm nestled amidst the flowing embrace of the Tigris and Euphrates rivers, now known as Contemporary Iraq. This ethereal land, replete with its idiosyncratic charm, demanded meticulous irrigation and adept drainage systems to unlock its agricultural potential. Within the fertile embrace of Mesopotamia, the indomitable spirit of early civilizations sprouted, fueling a relentless pursuit of ingenious flood control mechanisms, water reservoirs, and revolutionary irrigation practices [1]. The riverbank's stability is influenced by several factors, such as the riverbank's shape, soil characteristics, water pressure within the soil, the pressure from the water in the river, and the vegetation along the riverbank [2]. The riverbank's shape (geometry of the riverbank), including its inclining angle and height, is crucial in determining stability. Steeper angles of riverbank increase instability [3]. Soil characteristics, such as cohesion, internal friction, and erodibility, significantly impact stability. Cohesive soils offer more resistance, while erodible soils are prone to degradation. Hydraulic conditions encompass water level fluctuations and flow dynamics in the river [4]. Simon et al. [5] Sudden drawdowns can elevate positive pore water pressures and diminish cohesion, weakening the riverbank. In contrast, the negative pore water pressures cause an apparent cohesion and increase the stability of the riverbank. Also, vegetation is of significant importance for riverbank stability. However, it should also be viewed cautiously, as vegetation may interact with other factors, such as soil type and climate, and negatively affect the riverbank's stability [6]. The failure mechanism depends on the soil characteristics and riverbank geometry [7]. The cause of riverbank erosion is a significant issue for managing unstable rivers. Despite its many benefits, the riverbank may be unstable due to erosion and flooding, damage to the infrastructure, loss of property, and even loss of life. Therefore, effective riverbank management is essential for maintaining its functions while minimizing the risks associated with instability [8]. The failure mechanism depends on the soil characteristics and riverbank geometry [7]. The cause of riverbank erosion is a significant issue for managing unstable rivers. Failure of riverbanks can be caused by different reasons, including fluvial toe erosions, decreased soil shear strength caused by increasing pore water pressure in the soil, and seepage. Changes in the pore water pressure in the soil of the riverbank are considered one of the most important reasons leading to the collapse of the riverbank; as a result of these differences in pore water pressure during the periods of variables discharges of the river are the most important periods in determining the stability of the riverbanks and considered complex, rapid in occurrence and difficult to predict [9-11]. Unstable riverbanks can cause significant damage to infrastructure, such as bridges, roads, and buildings, as shown in Fig. 1. Riverbank instability can also increase sedimentation, degrade water quality, and harm aquatic [8]. A previous study showed that Tikrit City would be exposed to various flood scenarios [12]. Examining the riverbank's stability is crucial due to the potential risks of collapse due to expected floods and ensuring the safety of residents and vital structures along the riverbank. Therefore, the study aims to assess the stability of the riverbank through field investigations to ensure the riverbank stability for the Tigris River within the Salah Al-Din governorate by examining the safety factor

of the riverbank along the study area through careful analysis, which is essential to prevent potential problems instability in the riverbank that make the region safer for people and their surroundings.

Fig. 1 Collapse of Riverbank of Water Intake in the Study Area.

2.STUDY AREA AND DATA SOURCES

The Tigris River is a significant and vital waterway in the Middle East. Its source is in the Taurus Mountains range, situated in the southeastern part of Turkey. After completing its journey through the Turkish territory and then into the Syrian territory, the Tigris River enters Iraq in an area called Fishkhabour and continues its progress towards the south of the country, passing through numerous Iraqi cities and villages in the north, middle, and southern regions until reaching the Qurna area in Basra Governorate. There, it meets with the Euphrates River, and the two rivers merge to form another larger river called the Shatt al-Arab. The Shatt al-Arab River flows southward until it empties into the Arabian Gulf. As mentioned earlier, the Tigris River passes through many Iraqi cities and villages, including Salah Al-Din Governorate, with its center being the city of Tikrit. Due to the distinctive geographical location of Salah Al-Din Governorate, among other factors, numerous large-scale factories and plants have been established in this city, such as oil, electricity, and petrochemical projects. Because these projects require water, they have been built in locations close to the river's course, significantly impacting the nature of the river's water. This issue is evident through the increasing water demand, leading to the establishment of several water stations along its riverbanks, as well as its significant impact from industrial waste disposed of in it. Therefore, sustainable water resource management represents a critical challenge in facing changing conditions and the increasing water demand, encouraging more in-depth and specialized studies in this region of the river. In addition to Tikrit, several other districts in Salah Al-Din Governorate, like Baiji and Makhoul, are situated along the Tigris River riverbanks within the study area. These districts have important water projects located near the Tigris River. Therefore, it was crucial to inspect and ensure the safety and stability of the riverbank, starting from Makhoul and extending to Tikrit, to ensure the safety of these important facilities. The research area covers approximately (82) kilometers, extending from the Makhoul Dam in the north (upstream) to the Tikrit Bridge in the south (downstream) within Salah Al-Din Governorate. A total of 20 cross-sections were chosen along the Tigris River to comprehensively measure their dimensions, as illustrated in Fig. 2. Usually, significant fluctuations in the outflow of rivers occur during one year, so the Tigris River was monitored within the study area located from Makhoul to Tikrit for 2022, where the following data were recorded in the field: The discharge recorded a minimum value of 420 m^3/s and a maximum value of 1100 m^3/s. The width of the river is in the range (120-290)m, the max depth (3-9)m, the mean depth (2.15-6.37)m, the elevation of the water surface in the discharge of 515 m^3/sec (109.4 upstream–77.8 downstream)m, the elevation of the water surface in the discharge of (940)m^3/sec (110.31 upstream–79.69 downstream) m, the bed slope (s) 0.00038, the manning value after calibration 0.030, the velocity (0.53-1.36) m/sec, and the groundwater level in the riverbank is higher than the river water surface by (1-2) m.

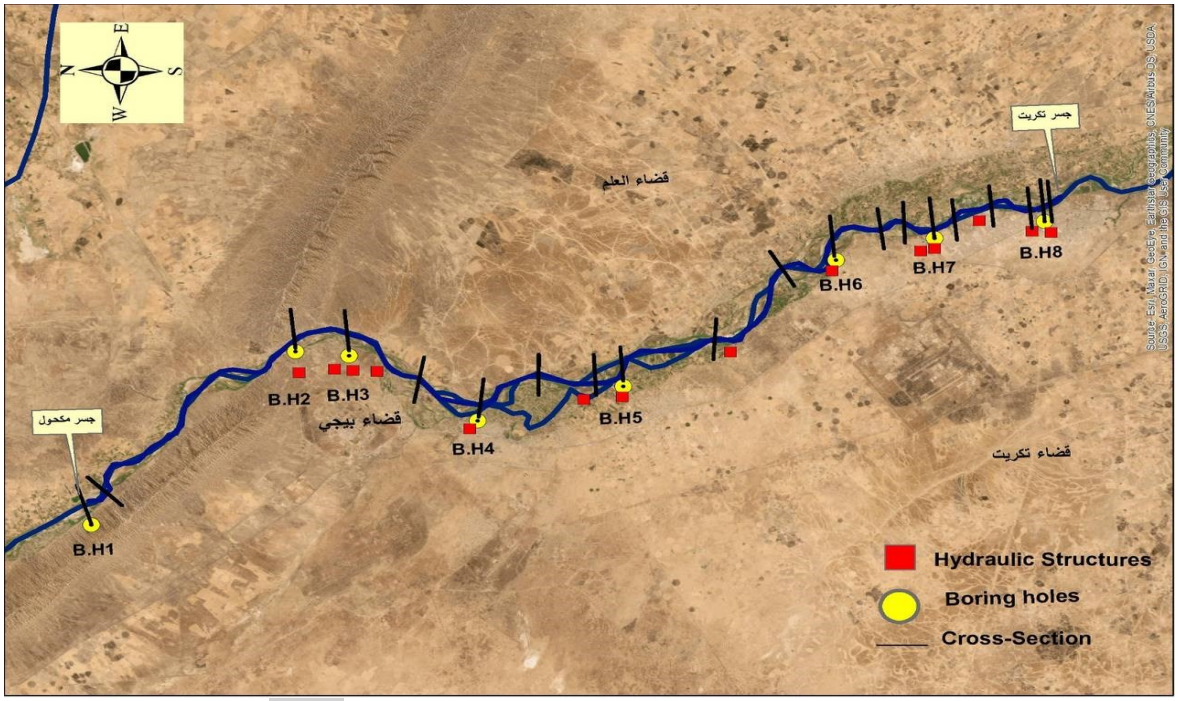

Fig. 2 The Reach of the Tigris River in the Study Area.

2.1. Cross Sections

Twenty cross-sections were selected within the Tigris River to conduct detailed measurements of their geometry. An Acoustic Doppler Current Profiler (ADCP) of the M9 type was used for measuring the river's discharge, velocity, and depth. With a full report on those details and creating profiles representing the river section between its riverbanks, it was necessary to set indicative markers to identify the sections whose geometry had to be measured again to perform second measurements at the same positions, as shown in Fig. 3. Additionally, a total station device type Topcon GTS225 with accuracy "1 second" was utilized to measure the riverbank's height and the water level within each section. The first observations were made through the indicative markers set at specified positions for all cross-sections. Second observations were made in the same sections to quantify the extent of change at the riverbed and assess the impact of deposition and erosion processes.

Fig. 3 The Indicative Markers for Cross-Section.

2.2.Geotechnical Characteristics of the Riverbank Soil

Soil boring samples were collected from eight points along the riverbank to examine the soil's physical characteristics and categorized by analyzing these soil boring samples. The boreholes were strategically placed as close as possible to the riverbank where the hydraulic structures were located to ensure precise data collection regarding the soil composition of the riverbanks. This approach aimed to observe any changes occurring in the soil layers and gather accurate information about the soil properties of the riverbanks. Boreholes were drilled using a hollow-stem auger, reaching a depth of 14 meters, as shown in Fig. 4. Table 1 lists the borehole locations and corresponding descriptions of soil distribution along the river.

Fig. 4 Soil Boring of Riverbank Along Tigris River.

Table 1 Soil Profiles Along Tigris River.

Borehole number	Area name	Borehole surface elevation (m)	Bottom elevation of layer (m)	Soil profile
B.H$_1$	Makhoul	110.98	106.98	GP
			100.98	SC-SM
			96.98	SM
B.H$_2$	Al-Fathaa	109	105	GP-GM
			99	SM
			95	ML
B.H$_3$	Shweash	107.6	103.6	SP
			93.6	GP
B.H$_4$	Baiji	108.2	94.2	GP
B.H$_5$	Al-Hejaj	98.73	96.73	GC
			94.73	SC
			92.73	CL
			84.73	GP
B.H$_6$	Al-Mahzam	92	90	SM
			88	SP
			86	SM
			84	GM
			78	GP
B.H$_7$	Tikrit University	87.97	85.97	GW
			81.97	SP
			73.97	GP
B.H$_8$	Tikrit	84.51	82.51	GP-GM
			78.51	SP-SC
			76.51	GM
			70.51	GP

where GP= Poorly graded gravel, Gw= Well-graded gravel, GM= Silty gravel, GC= Clayey gravel, SP= Poorly graded sand, SM=Silty sand, SC= Clayey sand, CL=clay, ML=Inorganic silt and fine rock flour with slight plasticity, SC-SM=Silty clayey sand, GP-GM= Poorly graded gravel with silt, and SP-SC= Poorly graded sand with clay. The river geometry and soil layers of the riverbank within the study area can be seen for cross-sections in Fig. 5.

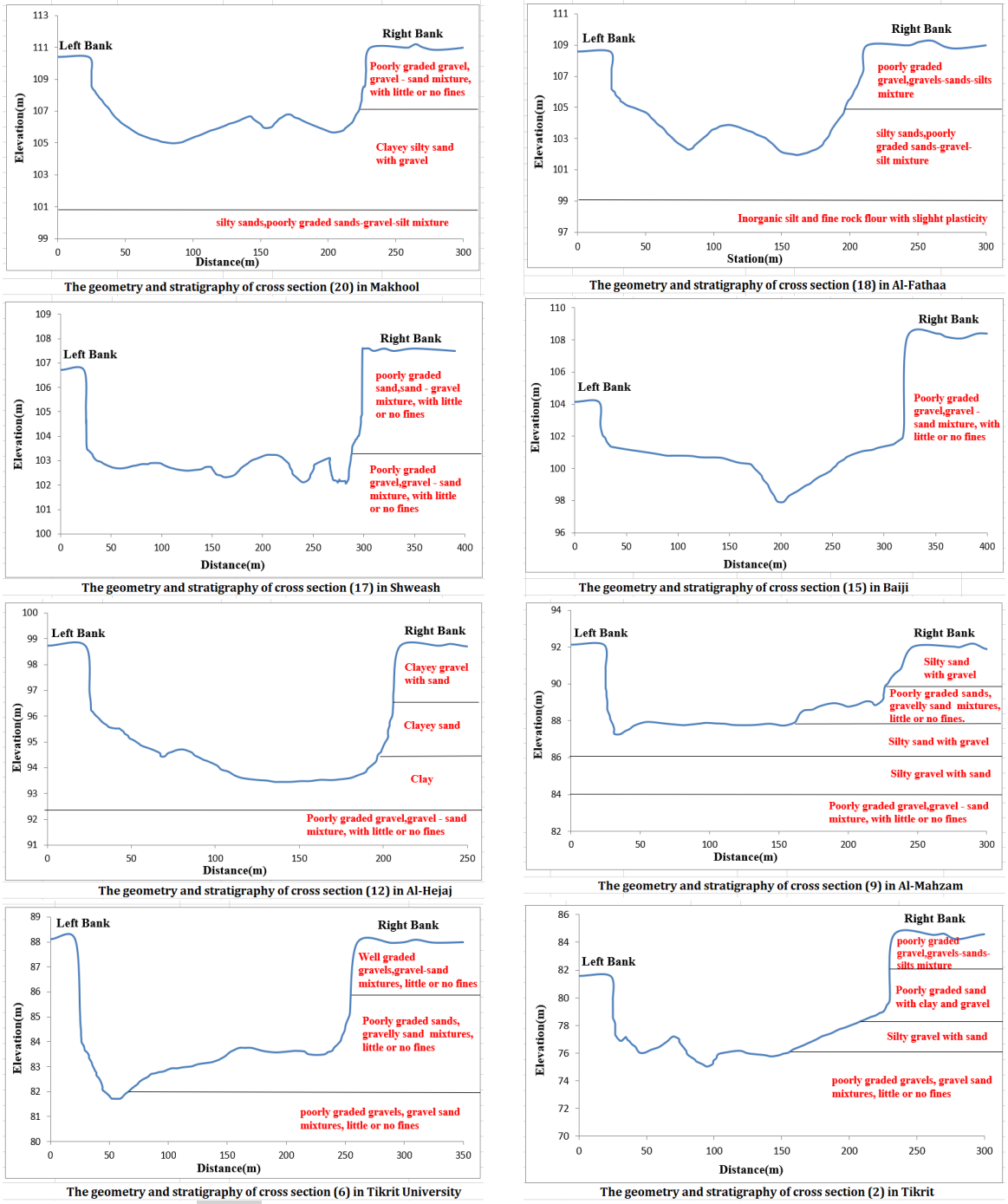

Fig. 5 The River Geometry and Soil Layers for the Riverbank.

2.3.Bed Material Samples

Samples were collected from the riverbed to obtain information regarding the properties of the bed material near the eight riverbank soil borings. A grab bucket sampler was utilized to collect samples of the upper layer of bed material from the riverbed. Bed material samples were collected using Van Veen Grabs with a volume capacity of 5.3 liters. Selecting sampling locations, sizes, and methods followed the guidelines classified by Fripp and Diplas [13]. Three samples were obtained from the surface and sub-surface layers at distances corresponding to 1/4, 1/2, and 3/4 of the average width for each cross-section [14]. The bed material samples collected were analyzed in the soil laboratory at Tikrit University. As shown in Fig. 6, the particle size distributions were determined using sieving analyses alone, without using a hydrometer for the surface layer samples. This approach was chosen as the percentage of fine materials passing through the 0.075 mm sieve was less than 10% for all tested samples. These results agree with those obtained by Nama et al. [15].

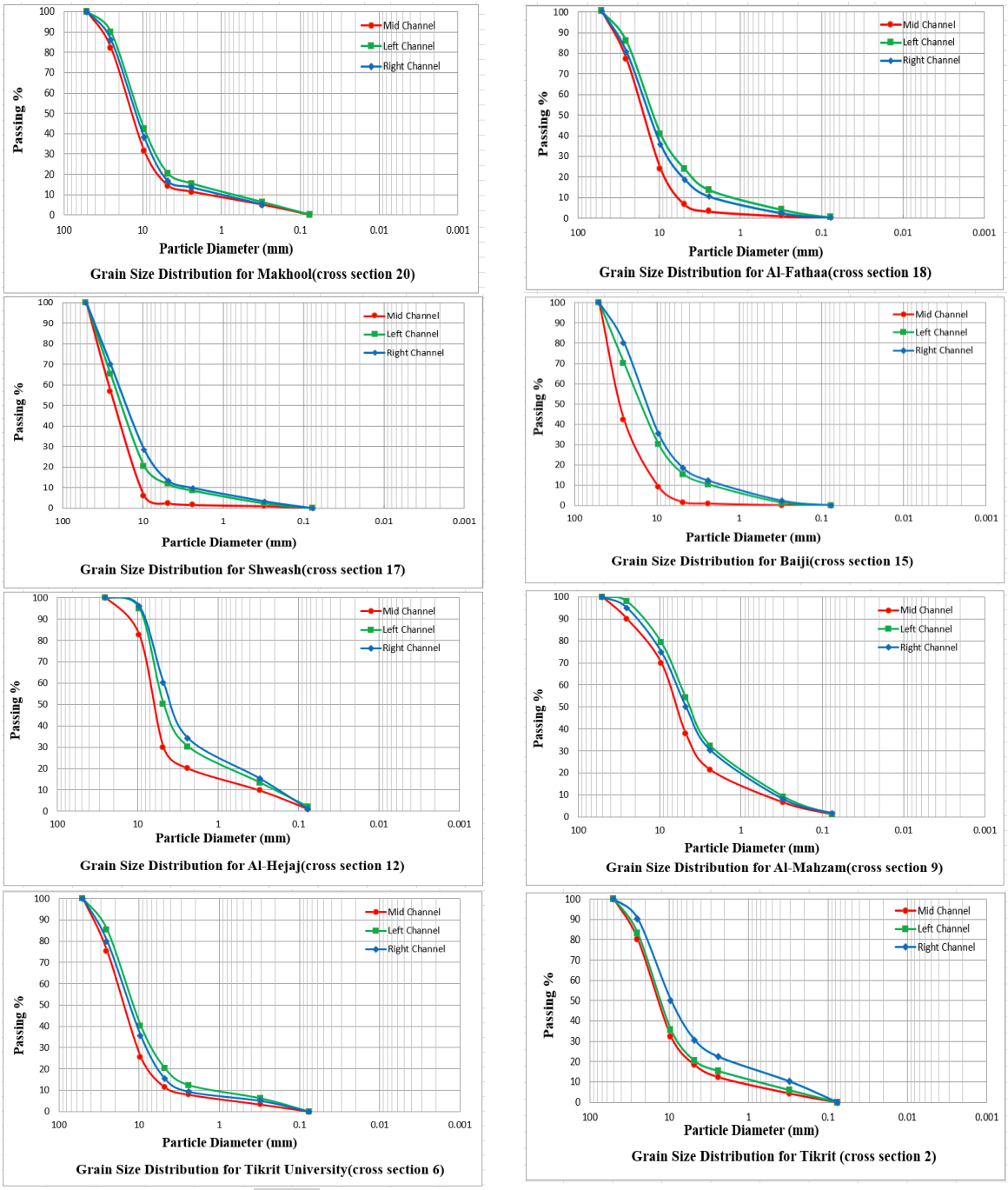

Fig. 6 Grain Size Distribution of the Bed Material.

2.4.Flow Data

The daily discharge data for the Tigris River within 2022, obtained from the Directorate of Water Resources-Salah Al-Din, can be used to create a typical outflow hydrograph. This hydrograph illustrates the variation in low and high flows over time and highlights how these changes can significantly affect the water surface elevation in different river sections**.** Figures 7 and 8 show the flow hydrograph of Biji and Al-Alam Guage. The present study ignored any data on lateral inflows for the Tigris River because data from the Directorate of Water Resources-Salah Al-Din found that the quantities of water withdrawn for water treatment stations accounted for approximately 3.84 m^3/sec, while irrigation stations were about 4 m^3/sec within the study area. However, no information was available regarding the delayed flow that reaches the river as groundwater flow (base flow). Consequently, the lateral inflows were deemed relatively insignificant compared to the overall discharge of the river due to the small amount of lateral inflow discharge compared to the flow in the river. Therefore, no data on tributary river flow was utilized in the present study. The data of water surface elevation for the Tigris River within 2022, obtained from the Directorate of Water Resources/Salah Al-Din, can be used to plot in the stage hydrograph, as shown in Figs. 9 and 10.

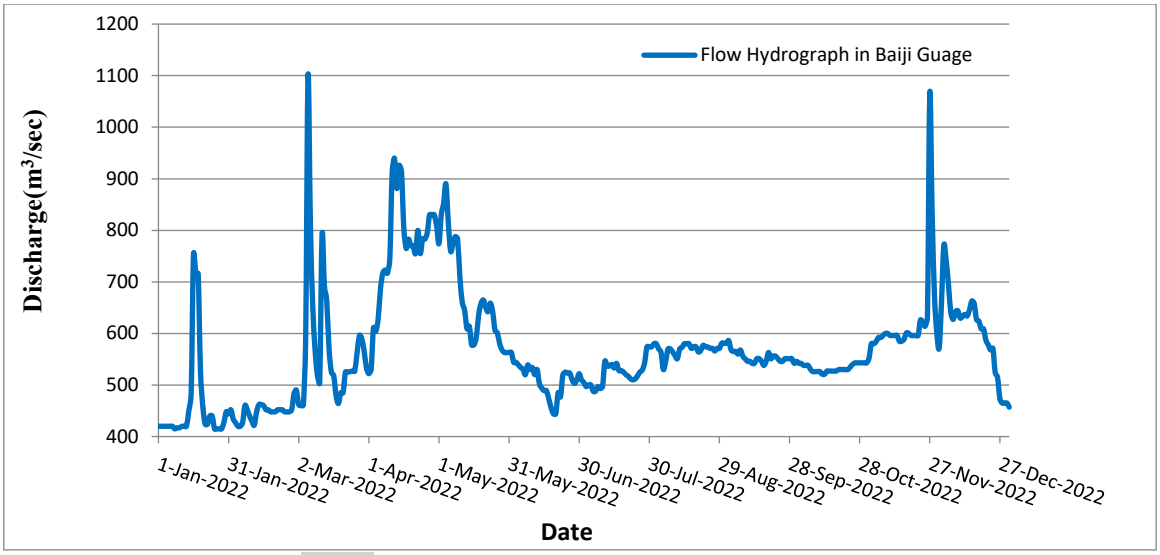

Fig. 7 Flow Hydrograph at Baiji Guage Station.

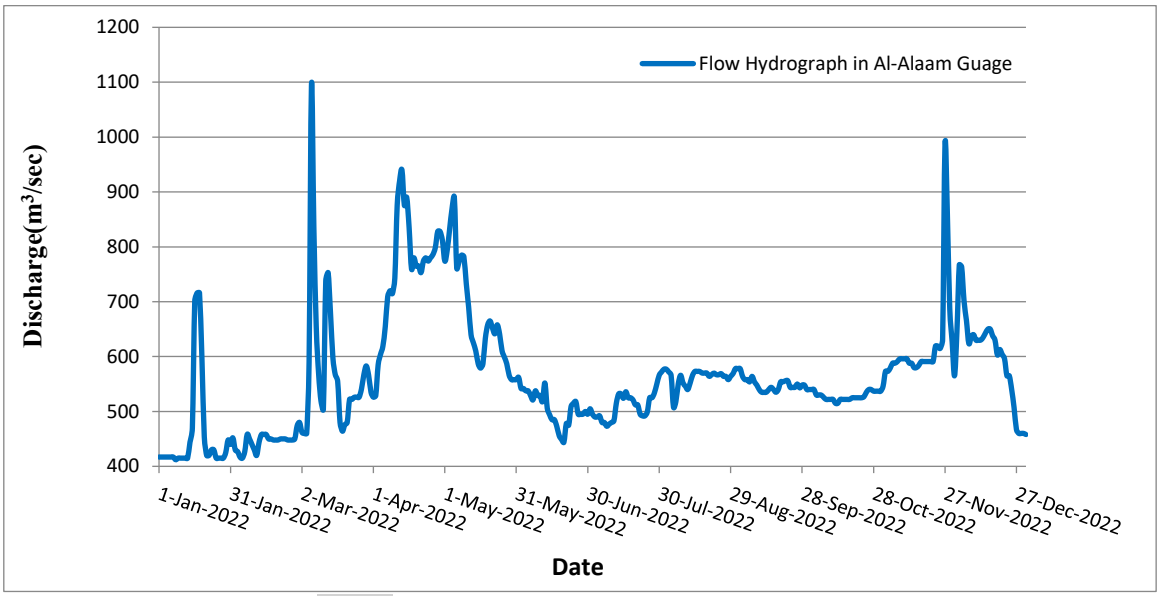

Fig. 8 Flow Hydrograph at Al-Alaam Guage.

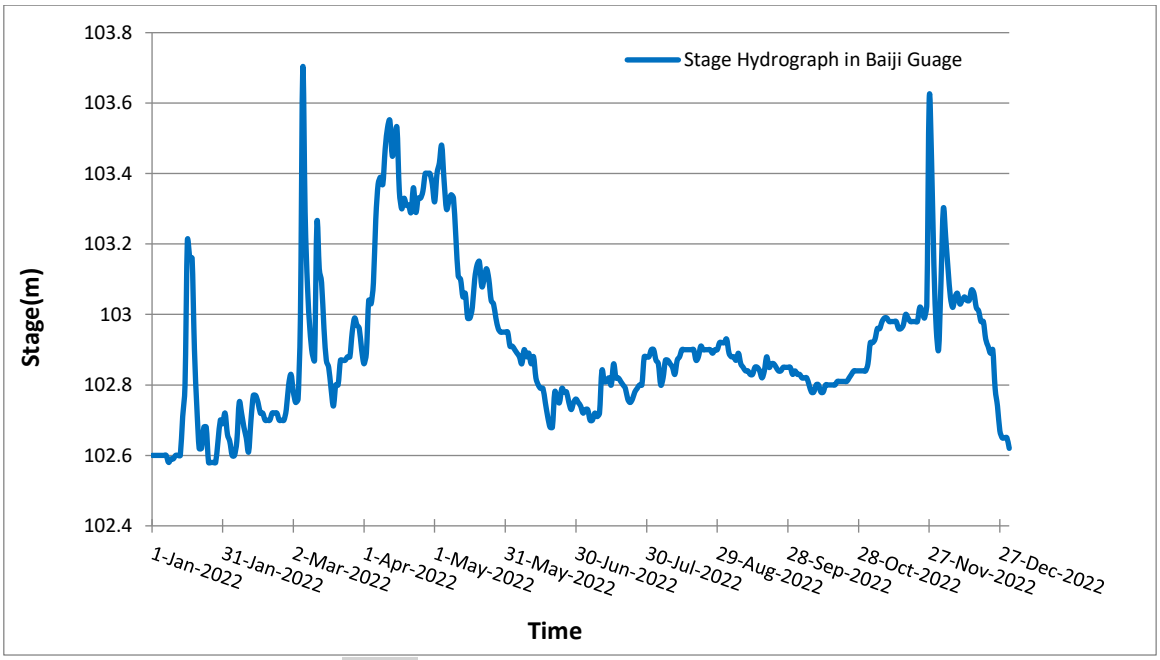

Fig. 9 Stage Hydrograph in Baiji Guage.

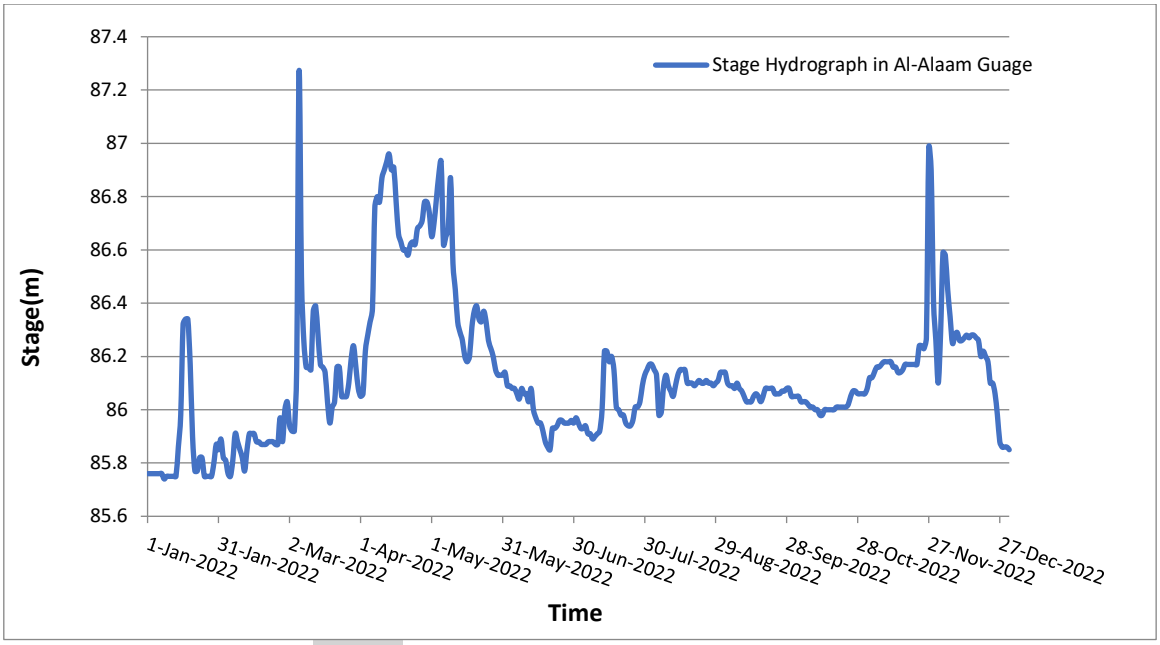

Fig. 10 Stage Hydrograph in Al-Alam Guage.

2.5.Groundwater Measurement

To determine the groundwater levels in the specified study area, particularly near the Tigris Riverbank, measurements were taken in various wells and compared with the water surface in the Tigris River simultaneously. Aecho Sounder device was employed to measure the water levels within the wells. At the same time, a Global Positioning System (Differential GPS System) was used to measure the elevation of the ground surface (wellhead) relative to sea level. This method assists in determining the groundwater level and finding a phreatic line through which saturated and unsaturated soil layers can be separated. This measurement was conducted using the Chc i90 device with an IMU-RTK GNSS receiver. This receiver integrates the features of two different types of GNSS receivers: an Inertial Measurement Unit (IMU) and a Real-Time Kinematic (RTK) receiver. This technology is utilized for applications that need extremely accurate positioning and orientation. This device includes a Continuously Operating Reference Station (CORS) technology, improving the accuracy level of the measurements. The accuracy of the vertical device was (1) cm, used in measuring levels, while its accuracy in measuring horizontal distances was between (2 and 3) cm. The measurements from the wells indicated that the groundwater level near the river, within a distance of (100 to 200) meters, had increased by approximately (1-2) m compared to the river level. For the wells located at distances of (0.9, 1.1, 2.2, and 2.5) kilometers from the river, the water level showed an increase of approximately (10, 13, 15, and 16) m, respectively, compared to the river's water level. Field measurements showed that the groundwater levels in the research region were higher than the river's water level, and the groundwater flow was in the river's direction (Gaining stream) [16, 17].

3.MODEL DESCRIPTION AND IMPLEMENTATION

The HEC-RAS program, i.e., Hydraulic Engineering Center- River Analysis System, was created and developed by the Corps of Engineers in the United States Army in Davis, California, Hydrologic Engineering Center. It is currently available to the public. It may be used to simulate steady flow (one-dimensional flow) and unsteady flow (one or two-dimensional flow), analyze the sediment transport across movable beds, and estimate water quality [18]. Hydraulic engineers can use the program to calculate flood plains and channel flows and assist in decision-making about essential issues influencing water courses. During unsteady flow conditions, the HEC-RAS software utilizes numerical methods to solve a complete set of 1-dimensional Saint-Venant equations. These equations consist of the continuity equation, derived from the principle of mass conservation, as well as the momentum equations. These governing equations define the behavior of the flow within the waterway.

$$\frac{\partial Q}{\partial X}+\frac{\partial A}{\partial t}-qi=0 \quad (1)$$

$$\frac{1}{A}.\frac{\partial Q}{\partial t}+\frac{1}{A}.\frac{\partial}{\partial x}\left(\frac{Q^2}{A}\right)+g.\frac{\partial y}{\partial x}-g(S_\circ-S_f)=0 \quad (2)$$

Q= discharge, y = flow depth, A = flow area, t is time, x = distance in the flow direction, g = acceleration due to gravity, S_o = bed slope, S_f = energy grade slope, and qi = lateral inflow. To address one-dimensional unsteady flow, the continuity equation Eq. (1) and the momentum equation Eq. (2) were solved mathematically using the four-point implicit box partial

differential scheme [19]. To obtain numerical results from HEC-RAS, users are required to input specific data. Figure 11 illustrates the files that need to be provided, including geometry, flow, and boundary condition files, to run HEC-RAS.

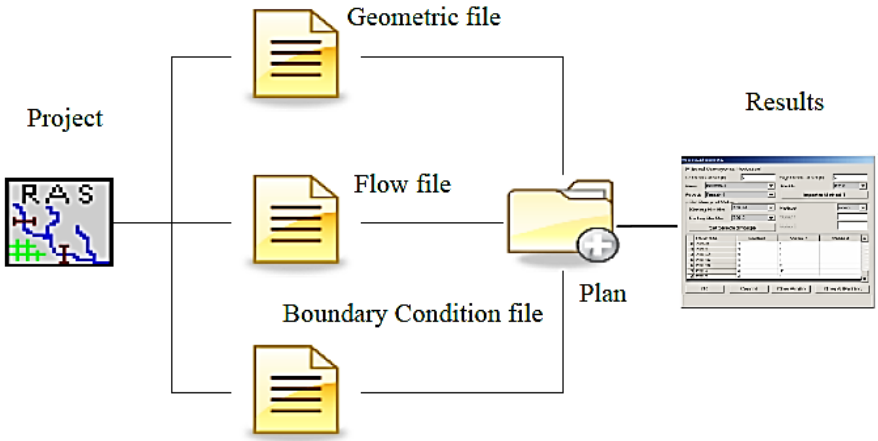

Fig. 11 Primary Input Data for HEC-RAS Software [19].

The main content of the geometric file primarily includes the data related to the cross-sectional geometry, representing the waterway within the designated study area. The flow file's content details the boundary conditions used in the simulations. The boundary condition file contains essential information for the simulation, including initial conditions at external boundaries (upstream and downstream) and interior cross-sections for unsteady and steady flows. The boundary condition upstream uses the discharge measured in the Baiji Gauge. Normal depth was used as a boundary condition downstream. Additionally, HEC-RAS can compute sediment transport by evaluating the sediment storage within the control volume by utilizing the sediment continuity equation, referred to as the Exner equation, i.e., Eq. (3).

$$(1-\lambda_p).B\frac{\partial \eta}{\partial t} = -\frac{\partial Q_S}{\partial x} \quad (3)$$

where λp represents the active bed layer porosity, B represents the channel width, η represents the bed elevation of the channel, t represents the time, Qs represents the transported sediment load, and x represents the distance. The sediment transport capacity was calculated using one of the sediment transport functions specified in the presented below according to Brunner's (2021): Acker-White, Engelund-Hansen, Laursen (Copeland), Meyer Peter Muller, Toffaleti, MPM-Toffaleti, Yang, and Wilcock-Crowe Brunner (2021). The eight equations employed for 1-D sediment transport functions and three additional transport functions (Soulsby-van Rijn, van Rijn, and Wu) are specifically designed for 2-D sediment transport functions. The most recent releases of HEC-RAS incorporate a new feature that enables the analysis of riverbank stability by implementing the Bank Stability and Toe Erosion Model (BSTEM). This model, developed by the USDA's National Sediment Laboratory and ARS, is a physically based approach that considers key processes like toe erosion and riverbank failure in layered or homogenous banks. The BSTEM was used in this context to compute the safety factor (SF) at various time points within a predefined outflow release scenario. The safety factor is defined as a ratio between the resisting force, which is a function of the strength of the soil forming the riverbank to the driving force, which is a function of the weight of the soil, its moisture, and the geometry of the riverbank [20, 21]. This safety factor concept measures the riverbank stability in Eq. (4).

$$SF = \frac{\sum_{m=1}^{M}\left(c'_m L_m + S_m \tan \emptyset_m{}^b + [W_m \cos\beta - U_m + P_m \cos(\alpha-\beta)] \tan \emptyset'_m\right)}{\sum_{m=1}^{M}(W_m \sin\beta - P_m \sin[\alpha-\beta])} \quad (4)$$

where m represents the number of layers, L represents the length of the failure plane, S represents the matrix suction force, W represents the weight of the soil block, U represents the Hydrostatic uplift, P represents the Hydrostatic confining force of the water in the channel, $\emptyset m'$ represents the friction angle, $\emptyset_m{}^b$ represents the relationship between matrix suction and apparent cohesion, c' represents the effective cohesion, β represents the failure plane angle, and α represents the channel side slope angle.

4.CALIBRATION AND VALIDATION OF THE MODEL

To ensure accurate flow calculations and account for uncertainty, it is crucial to calibrate and validate the models used in any study. In this research, the discharge data was measured from January to July 2022 and utilized for calibration. Manning's Roughness Coefficient

(n) was adjusted along the Tigris River within the study area to match the water surface elevation and river discharge at the Baiji gauge. Multiple values of Manning's coefficient (n) were tested to assess their impact on the accuracy of the flow simulation results in the study area. Following the calibration process, the final range of Manning's coefficient (n) was determined to be (0.026-0.033), with an average value of 0.03 observed across most sections of the Tigris River within the Salah Al-Din Governorate. These results agree with those obtained by [22, 23]. Also, this value is within the limits of the Manning coefficient indicated in the source [24]. The comparison between the values of Manning's coefficient (n) used in the model and the readings from the AL-Alam gauge indicated that the performance of the HEC-RAS model was consistent and satisfactory. Figure 12 compares the daily river flow values obtained from the AL-Alam gauge with the predicted values generated by the HEC-RAS model during the calibration period from January to July 2022. The high level of agreement between the observed and predicted values validates using Manning's coefficient (n) for model calibration, providing confidence in the model's accuracy.

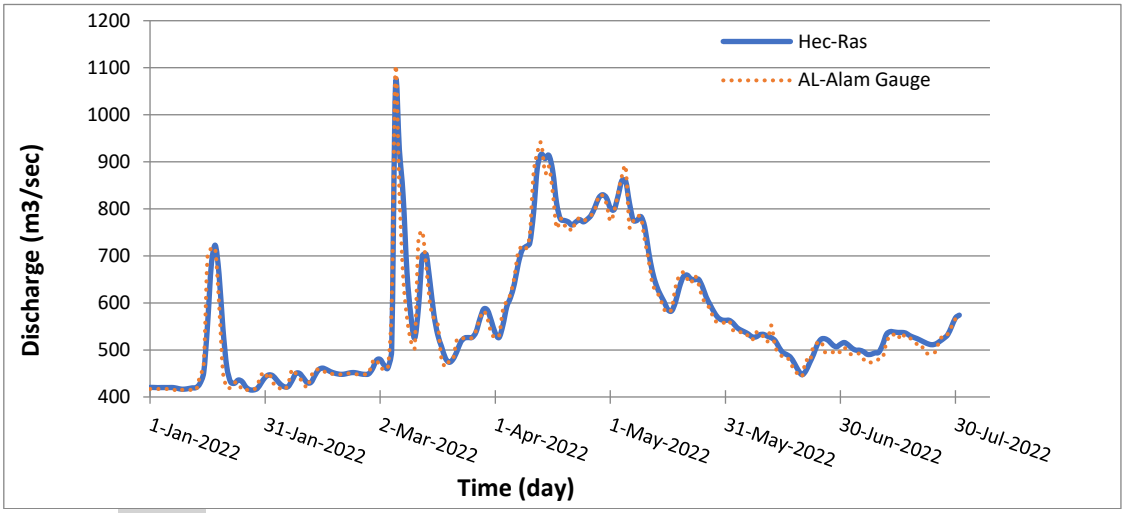

Fig. 12 Flow Comparisons of HEC-RAS and AL-Alam Gauge Jan–Jul 2022.

A validation process was conducted to evaluate the effectiveness of the calibrated HEC-RAS model. The Tigris River flow hydrograph data from August to December 2022 were employed as the validation dataset. The hydraulic flow results obtained from the calibrated HEC-RAS model exhibited behavior and performance that aligned well with the measured flow values from the AL-Alam gauge. This correlation between the model predictions and the observed flow values indicates the suitability and reliability of the calibrated HEC-RAS model for accurately simulating the flow dynamics of the Tigris River. Figure 13 shows the recorded flow data from the AL-Alam gauge during the selected validation period compared to the flow results obtained from the HEC-RAS model.

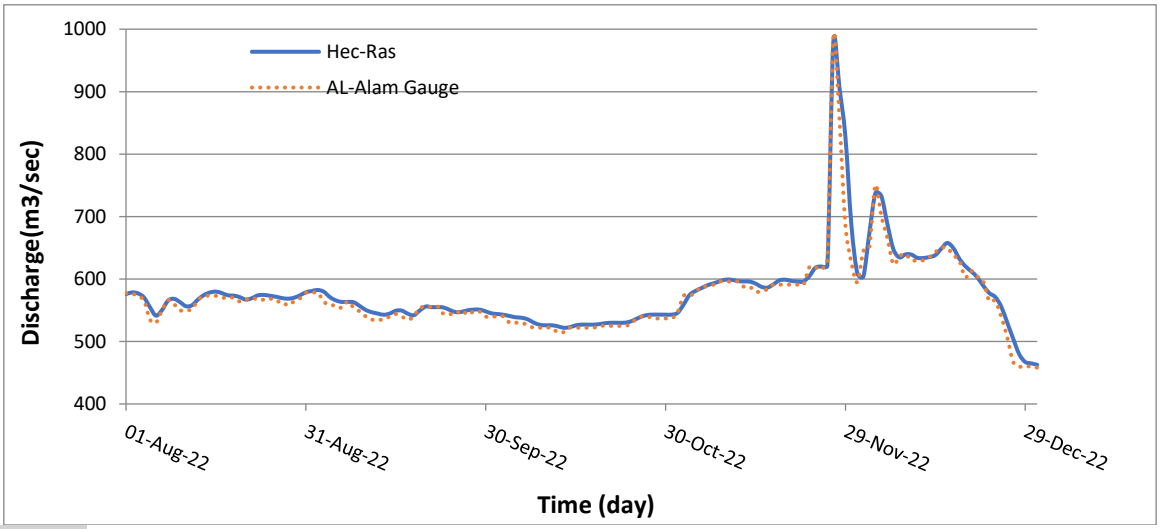

Fig. 13 Compares the Recorded Flow at the AL-Alam Gauge to the HEC-RAS Model Findings from the Previously Selected Validation Period.

In addition to determining the effectiveness of models, one of the most trusted and well-known methods is the Nash-Sutcliffe Efficiency measure (NSE). The Nash-Sutcliffe Efficiency (NSE) measure, introduced by Nash and Sutcliffe in 1970 [25], is widely recognized as one of the most reliable and commonly used methods to assess the effectiveness of models; measuring serves as a quantitative indicator to evaluate the performance of models by comparing simulated values to observed values. The NSE measure provides valuable insights into the accuracy and reliability of models in replicating the observed data, thus serving as a trusted method in model evaluation. To assess the consistency between the model and the data, a statistical analysis was conducted to determine the level of agreement. Table 2 displays the main variables used in this statistical data analysis.

Table 2 Values of the Main Parameters of the Statistical Data Analysis.

Parameters	The Calibration Period	The Validation Period
R^2	0.9926	0.9881
Standard Error (m^3/sec)	11.48	4.58
NSE	0.986	0.976

In addition, the Implicit Weighting Factor (Theta) in HEC-RAS is a parameter used in unsteady flow analysis to determine the balance between the explicit and implicit components in the numerical solution. It represents the time-weighting factor that influences the contribution of each component. The recommended range for theta in HEC-RAS is typically between 0.6 and 1 [19]. The choice of theta depends on the desired balance between stability and accuracy. A higher theta value of 1 prioritizes accuracy; however, it may require smaller time steps. A lower theta value of 0.6 enhances stability; however, it may sacrifice some accuracy. It is essential to consider the specific characteristics of the river system being analyzed and conduct sensitivity analyses to determine the optimal value for a particular modeling scenario. The optimal value of theta for the present study was 0.8.

5.RESULTS AND DISCUSSION

The impacts of different discharge levels were assessed by calculating safety factors at multiple cross-sections. Eight identified cross sections (20, 18, 17, 15, 12, 9, 6, and 2) were selected along the Tigris River because they are strategically positioned in important areas within the study area, in the location where the hydraulic structures as close as possible to the river. These selected cross-sections also represent the various soil types within their respective reaches. The selection aimed to encompass significant locations along the Tigris River, considering hydraulic features and soil characteristics for comprehensive analysis. Essential data, including the geometrical characteristics of each cross-section, soil properties, and the water hydrographs, have been supplied to ensure the proper functioning of the model. These provided data are crucial for accurate simulations and analyses related to the study. These cross-sections represented the simulated riverbank safety factors under various discharge conditions in 2022. The calculated safety factor indicates that the riverbank is stable whenever its value is more than 1.3; when its value is between (1-1.3), the riverbank is conditionally stable and is considered unstable when it is less than 1 [26]. This criterion allows for a straightforward determination of the stability status of each cross-section along the Tigris River. Figures 14 to 21 show the relationship between discharge and safety factors at the selected cross-sections. Table 4 shows the safety factor values for the cross-sections in the study area with different discharges within 2022.

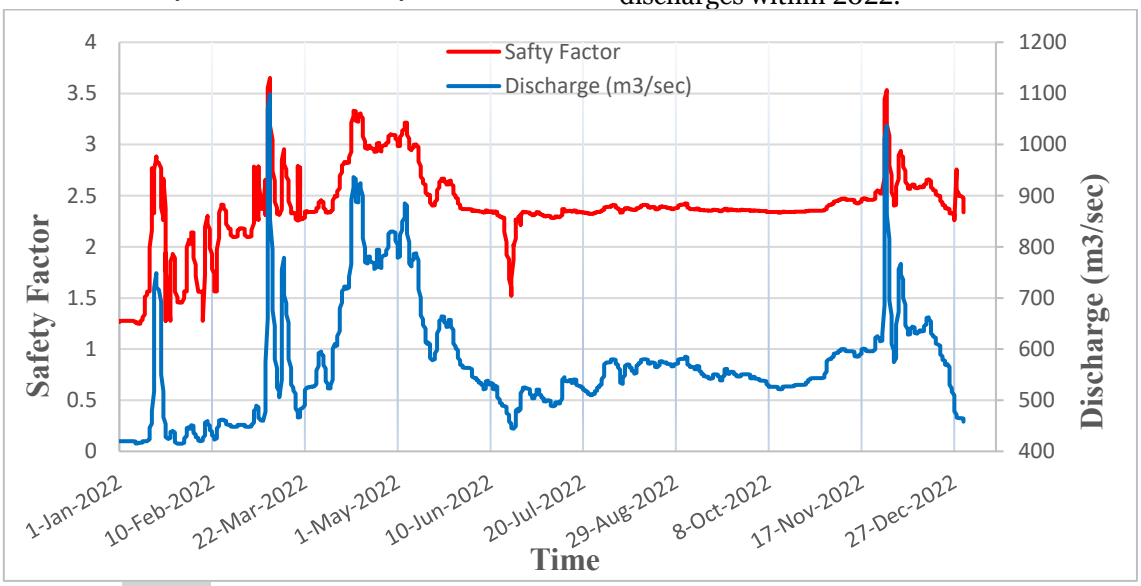

Fig. 14 Predicted Safety Factor in Section (20) Versus Discharge (Makhoul).

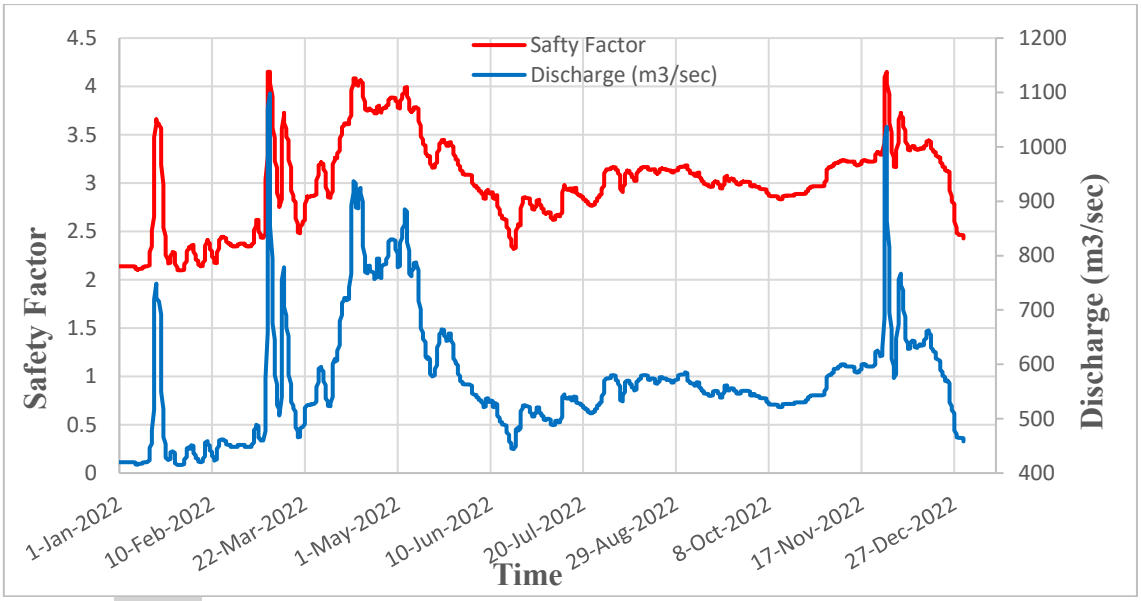

Fig. 15 Predicted Safety Factor in Section (18) Versus Discharge (AL-Fathaa).

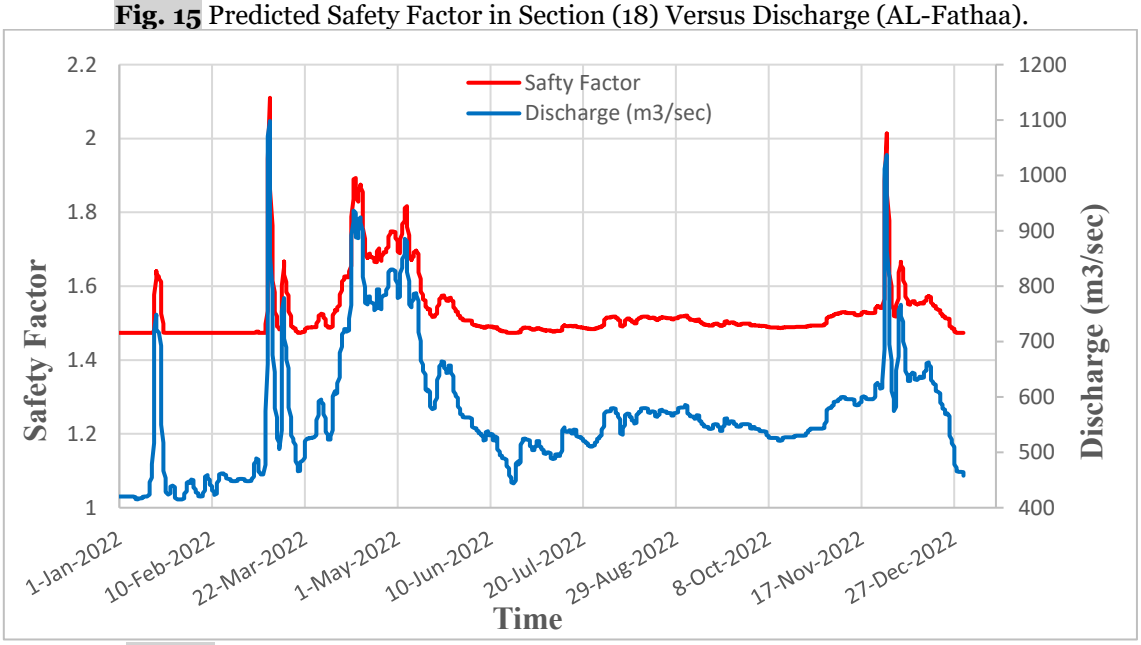

Fig. 16 Predicted Safety Factor in Section (17) Versus Discharge (Shweash).

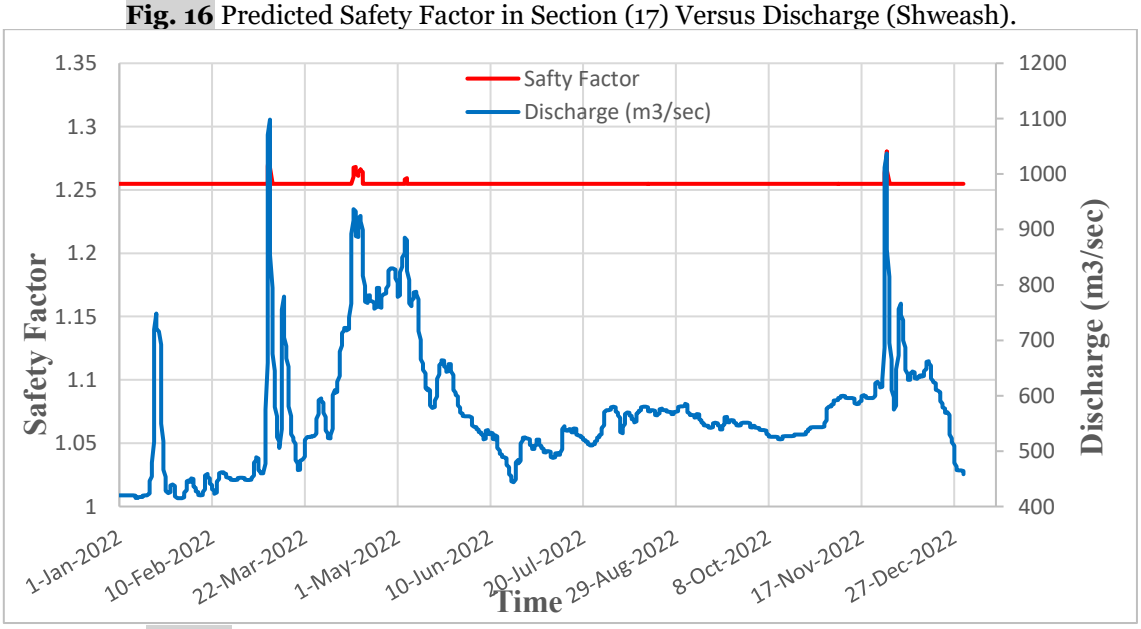

Fig. 17 Predicted Safety Factor in Sections (15) Versus Discharge (Baiji).

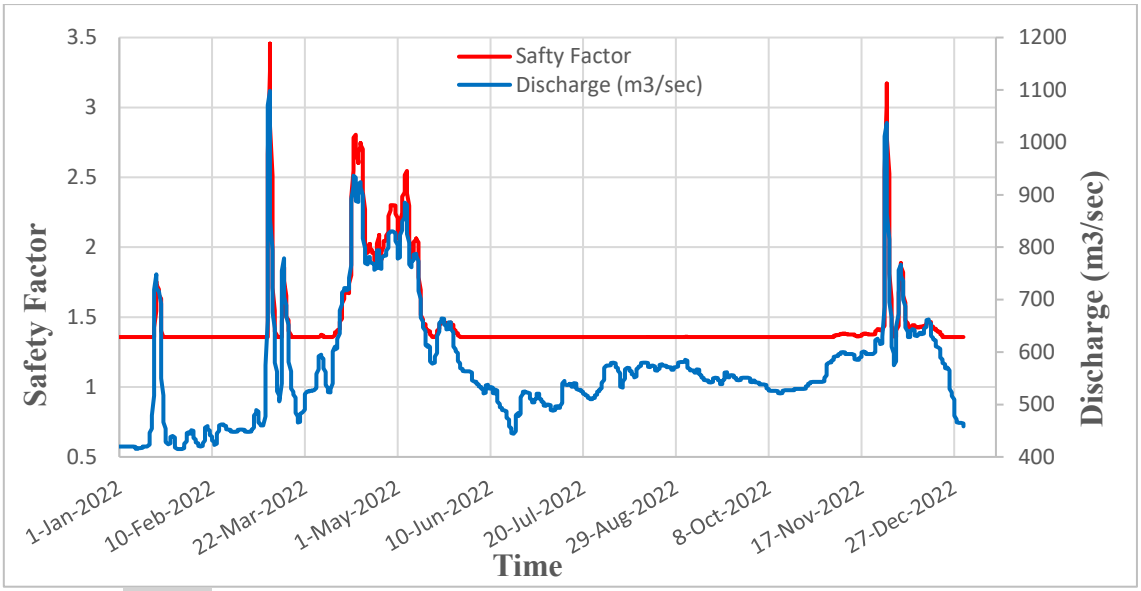

Fig. 18 Predicted Safety Factor at Section (12) Versus Discharge (AL-Hejaj).

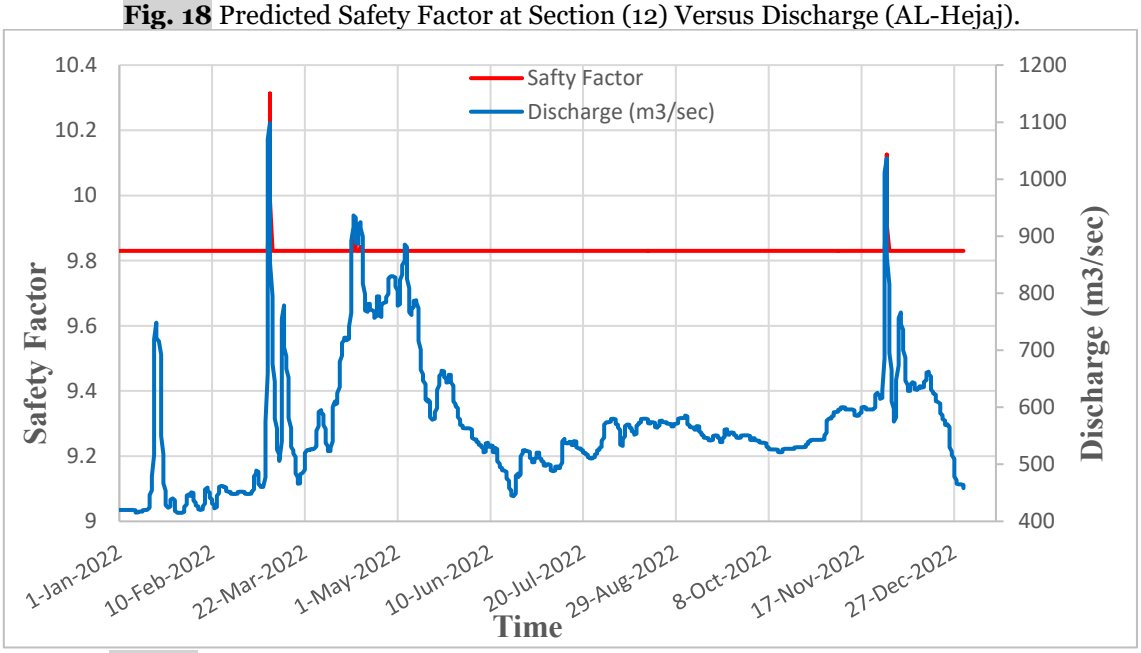

Fig. 19 Predicted Safety Factor in Section (9) Versus Discharge (AL-Mahzam).

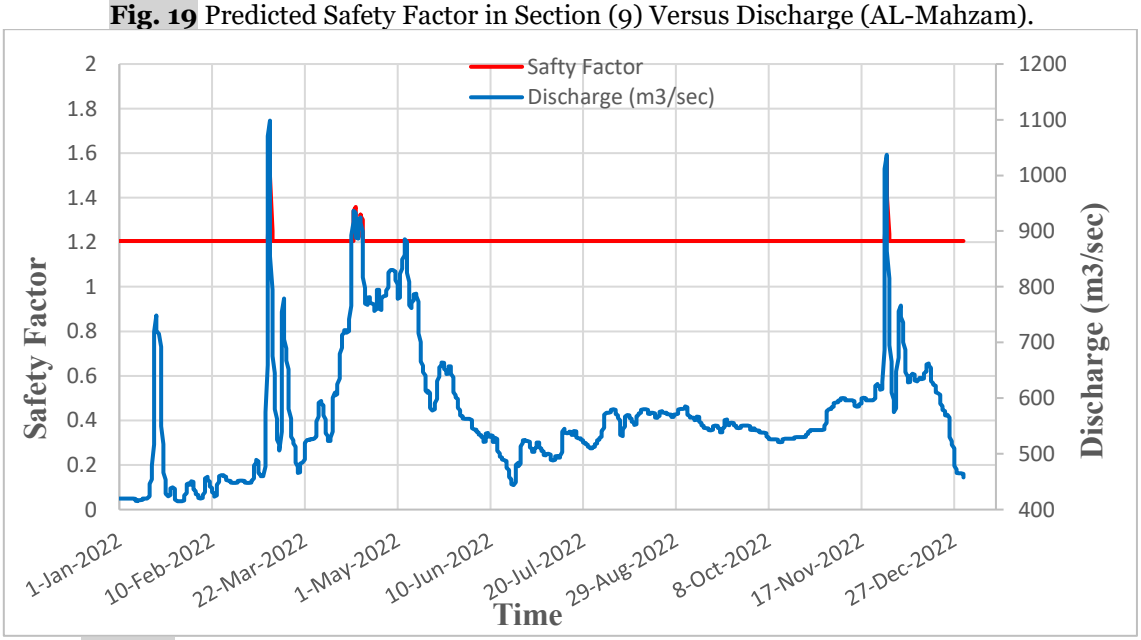

Fig. 20 Predicted Safety Factor in Section (6) Versus Discharge (Tikrit-University).

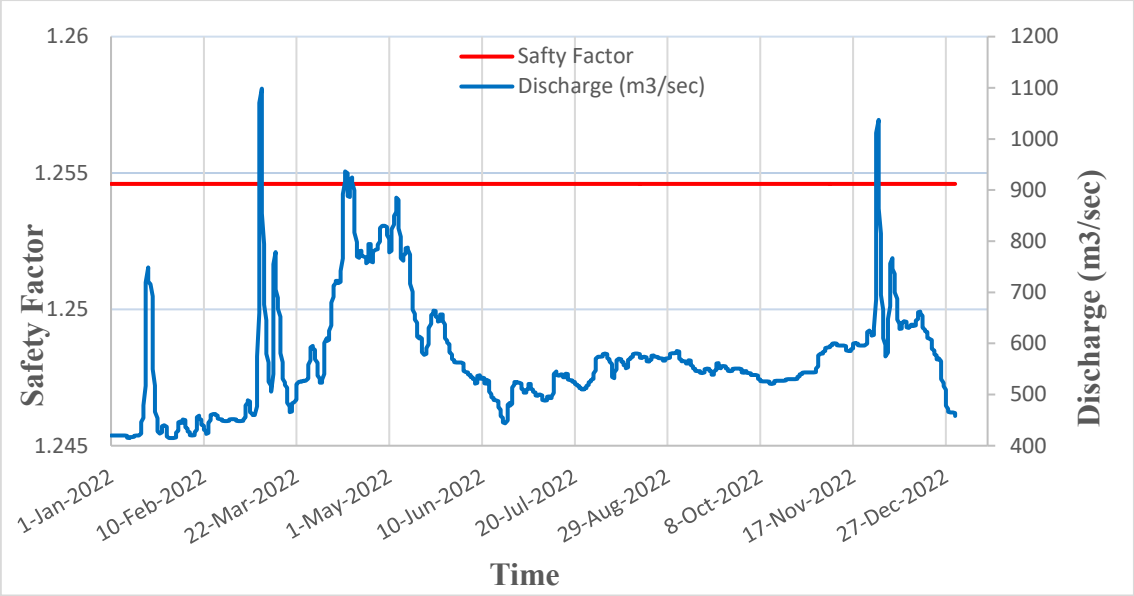

Fig. 21 Predicted Safety Factor in Section (2) Versus Discharge (Tikrit).

Table 3 Values of the Safety Factor with the Condition of Riverbank.

Cross section no.	Safety factor (SF)		Condition of riverbank
	Q_{max}=1100 m³/sec	Q_{min}=420 m³/sec	
20	3.65	1.2	Stable Conditionally Stable
18	4.1	2.12	Stable Stable
17	2.11	1.49	Stable Stable
15	1.28	1.25	Conditionally Stable Conditionally Stable
12	3.45	1.35	Stable Stable
9	10.31	9.83	Stable Stable
6	1.74	1.2	Stable Conditionally Stable
2	1.254	1.254	Conditionally Stable Conditionally Stable

The BSTEM program results showed that the study area's safety factor exceeded 1. The safety factor increased with a high flow of 1100 m³/sec. It was greater than 1.5 except in Baiji, i.e., 1.28, and Tikrit, i.e., 1.254. These safety factors mean that these two sections were conditional stability, while in the case of low flow 420 m³/sec, the safety factor recorded 1.2 in Makhoul, 1.25 in Baiji, 1.2 in Tikrit University, and 1.252 in Tikrit, i.e., these stations are conditional stability. The change in the safety factor with varying discharge levels highlights how the river's flow rate influences the stability of the cross-section. The change in the Tigris River's discharge value at most cross-sections impacts the calculated safety factor. All cross sections were stable when the resisting forces were greater than the driving forces; this resulted from good soil properties (C, Ø) and good riverbank geometry, such as a suitable height, mild slope, the presence of vegetation on the riverbank, and good confining pressure of the river's flow. High river flow affects the soil properties, increasing (C, Ø) while maintaining the same values of other parameters, such as riverbank geometry and vegetation. The confining pressure generated by the river water contributes to the support of the riverbank, generating a higher safety factor, which is shown in cross-sections (20, 18, 17, 12, 9, and 6). While the safety factor for the same cross-sections decreased with lower flow values due to the decrease in confining pressure and the change in soil properties. As for cross-sections (15 and 2), the high level of the riverbank made the effect of confining pressure non-existent, even with increasing the river flow. In these cross-sections (15 and 2), the safety factor was constant despite differences in flow conditions. It depends on the soil properties and riverbank geometry, which insignificantly changed in these sections with flow variations. Therefore, as long as the shear force, the weight of the soil, and the geometry of its riverbank remain relatively constant, the safety factor should also remain relatively constant with different flow conditions. Also, the result showed no change in the river bed, which means that the river bed reached the armoring bed, as shown in Figs. 22-24.

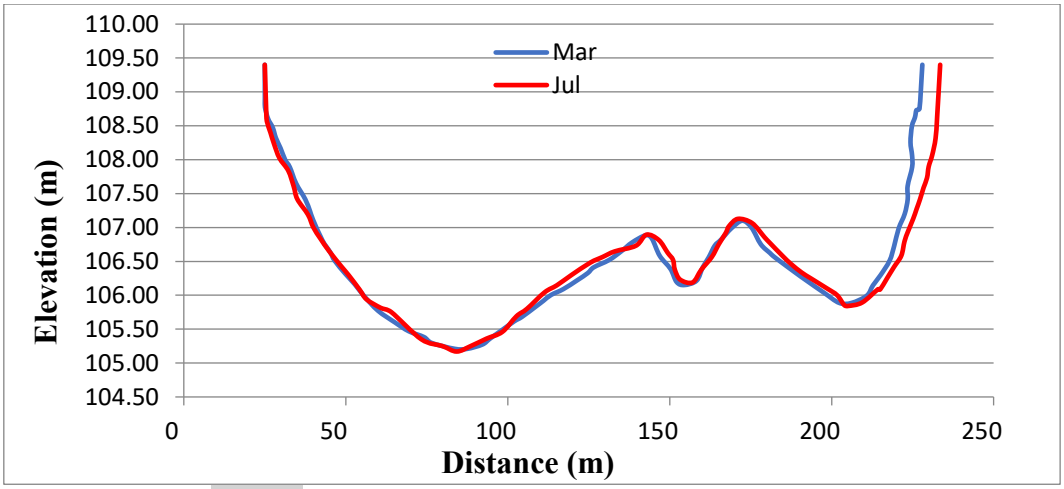

Fig. 22 Bed Geometry in Cross-Section 20 (Makhoul).

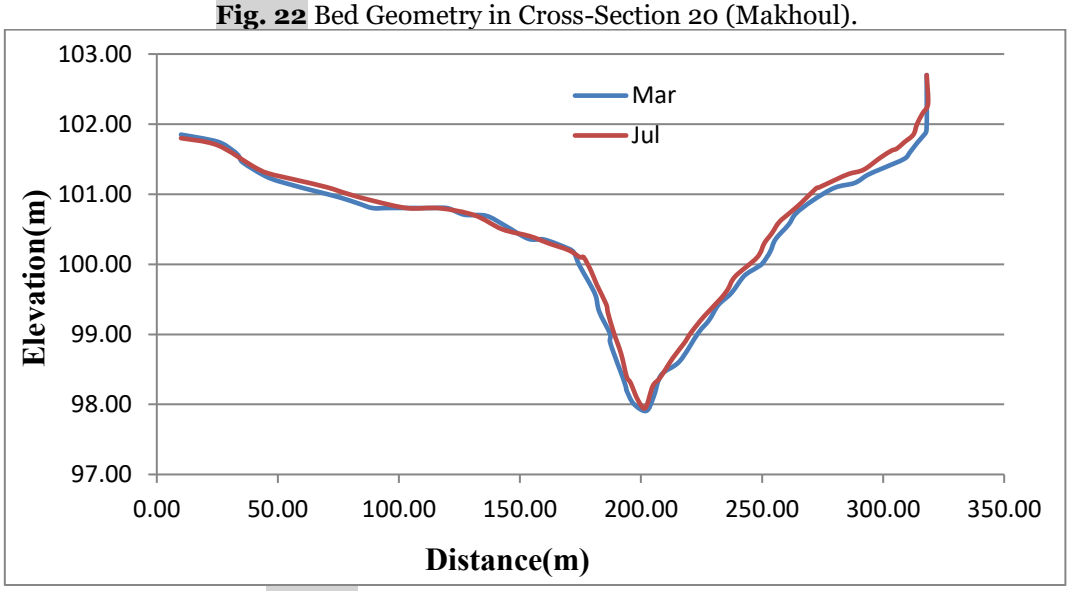

Fig. 23 Bed Shape in Cross-Section 15 (Baiji).

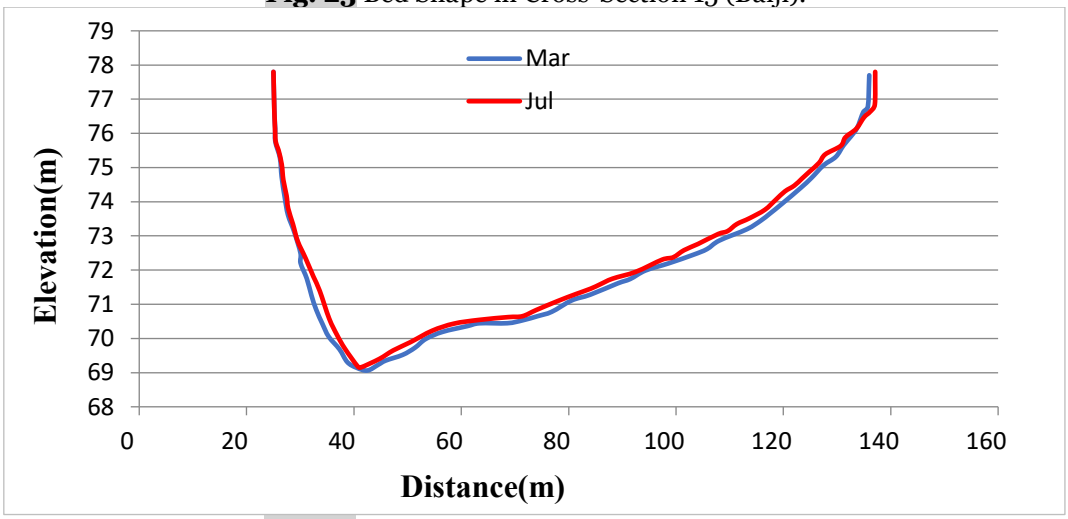

Fig. 24 Bed Shape in Cross-Section 2 (Tikrit).

6. CONCLUSIONS

The impact of discharge changes on the stability of the riverbank was examined over an 82-kilometer stretch of the Tigris River. Data obtained from field investigations to verify Tigris River bank's stability was customized for use in the integrated BSTEM model with the HEC-RAS model. Using data for flow events in (2022) from the Directorate of Water Resources/Salah Al-Din, the HEC-RAS model's 1-dimensional sediment transport and unsteady flow were accurately calibrated and verified. The simulation study findings gave enough details to locate the riverbanks in danger of a decreased safety factor caused by flow fluctuations. The findings showed that

variations in flow, riverbank geometry, riverbank slope, groundwater table level, and soil properties for each cross-section affected the computed safety factor (SF). All cross-sections were stable. However, some were conditional stability, and some remained constant safety factors without change, even when the river's water level varies. The constancy of the safety factor across different flow conditions was attributed to the consistent properties of the soil and the riverbank's geometry, which insignificantly changed with varying flow rates. These stable characteristics of the soil and riverbank geometry contributed to the cross-section's ability to maintain conditional stability, implying that it can withstand the prevailing forces. However, close monitoring and measures may be required to ensure stability, especially during different flow conditions.

7.RECOMMENDATIONS

While the dataset used in this study was fairly accurate, enhancing the model's precision could be achieved by acquiring more comprehensive field data. Gathering detailed information on the water table, specifically in alignment with the fluctuations in water surface elevation, can significantly improve the reliability of the stability analysis conducted on the Tigris River. This goal could be accomplished by installing piezometers at various cross-sectional points along the riverbanks, facilitating continuous monitoring of water table levels and surface elevations. An alternative approach for further investigation is utilizing a two-dimensional morphodynamic model. Utilizing a two-dimensional morphodynamic model holds significant potential as a beneficial instrument for examining riverbank evolution, particularly in light of their exposure to temporal variations in water level. Utilizing a two-dimensional morphodynamic model would address the constraints encountered in one-dimensional morphodynamic models with respect to generating planform evolutions, including width adjustment and meander bend migration. The Tigris River riverbanks' stability can be studied in the same area to evaluate the impact of the construction of the Makhoul Dam on the shape and stability of the riverbank after constructing the dam and to compare the results achieved from constructing the dam.

ACKNOWLEDGEMENTS

The authors are grateful for the support of this research by the Department of Civil Engineering, College of Engineering, Tikrit University. The university order number for admission to doctoral studies is 2732/3/7 on 2020/2/13. They also would like to acknowledge the help and guidance provided by Dr. Wesam Sameer Mohammed-Ali from the Environmental Engineering Department, College of Engineering, Tikrit University, during the preparation of this research.

REFERENCES

[1] Roberson JA, Cassidy JJ, Chaudhry MH. **Hydraulic Engineering.** *John Wiley & Sons*; 1998.

[2] Langendoen EJ, Simon A, Curini A, Alonso CV. **Field Validation of an Improved Process-Based Model for Streambank Stability Analysis.** *International Water Resources Engineering Conference 1999, ASCE*; 1999.

[3] Jha S, Western A, Rutherfurd I, Grayson R. **Testing Uncertainty in a Model of Stream Bank Erosion.** *MODSIM 2005 International Congress on Modeling and Simulation Society of Australia and New Zealand*; 2005:27714-22720.

[4] Mohammed-Ali W, Mendoza C, Holmes RR. **Influence of Hydropower Outflow Characteristics on Riverbank Stability: Case of the Lower Osage River (Missouri, USA).** *Hydrological Sciences Journal* 2020; **65**(10):1784-1793.

[5] Simon A, Curini A, Darby S, Langendoen E. **Streambank Mechanics and the Role of Bank and Near-Bank Processes in Incised Channels.** *Incised River Channels* 1999; **1**(999):123-152.

[6] Gray DH, Leiser AT. **Biotechnical Slope Protection and Erosion Control.** *Van Nostrand Reinhold Company Inc.*; 1982.

[7] Thorne CR, Osman AM. **Riverbank Stability Analysis. II: Applications.** *Journal of Hydraulic Engineering* 1988; **114**(2):151-172.

[8] Johnson MF, et al. **Biomic River Restoration: A New Focus for River Management.** *River Research and Applications* 2020; **36**(1):3-12.

[9] Hooke JM. **An Analysis of the Processes of River Bank Erosion.** *Journal of Hydrology* 1979; **42**(1-2):39-62.

[10] Thorne C. **Processes and Mechanisms of River Bank Erosion.** *Gravel-Bed Rivers* 1982:227-271.

[11] Wolman MG. **Factors Influencing Erosion of a Cohesive River Bank.** *American Journal of Science* 1959; **257**(3):204-216.

[12] Mohammed-Ali R. **Flood Risk Analysis: The Case of Tigris River (Tikrit/Iraq).** *Tikrit Journal of Engineering Sciences* 2023; **30**(1):112-118.

[13] Fripp JB, Diplas P. **Surface Sampling in Gravel Streams.** *Journal of Hydraulic Engineering* 1993; **119**(4):473-490.

[14] Laronne JB, Reid I, Yitshak Y, Frostick LE. **The Non-Layering of Gravel Streambeds under Ephemeral Flood Regimes.** *Journal of Hydrology* 1994; **159**(1-4):353-363.

[15] Nama AH, Abbasa AS, Maatooqa JS. **Hydrodynamic Model-Based Evaluation of Sediment Transport Capacity for the Makhool-Samarra Reach of Tigris River.** *Engineering and Technology Journal* 2022; **40**(11):1573-1588.

[16] Al-Kaisy SA. **Hydrogeological Conditions of Ajil Sub-Basin North of Iraq.** *College of Science, University of Baghdad*; 1992.

[17] Reem MJ. **Effect of Variation of Sedimentological and Textural Facies on the Hydraulic Properties of Unconfined Aquifer, Baiji City North of Iraq.** *College of Science, University of Tikrit*; 2015.

[18] Mohammed-Ali R. **Review for Some Applications of Riverbanks Flood Models.** *IOP Conference Series: Earth and Environmental Science* 2022: **1120**(1): 012039.

[19] Brunner GW. **HEC-RAS River Analysis System: Hydraulic Reference Manual, Version 6.0.** *US Army Corps of Engineers-Hydrologic Engineering Center*; 2021.

[20] Duan JG. **Analytical Approach to Calculate Rate of Bank Erosion.** *Journal of Hydraulic Engineering* 2005; **131**(11):980-990.

[21] Simon A, Curini A, Darby SE, Langendoen EJ. **Bank and Near-Bank Processes in an Incised Channel.** *Geomorphology* 2000; **35**(3-4):193-217.

[22] Nama AH, Abbas AS, Maatooq JS. **Investigation of the Morphologic Aspects for the Tigris River Reach between Makhool Dam and Samarra Barrage.** *Civil Engineering Department, University of Technology*; 2023.

[23] Kalaf HA. **Hydrological Study of a Section of the Tigris River between Shirqat District and the Lower Zab Estuary Using HEC-RAS Program.** *Midad AL-Adab Refereed Quarterly Journal* 2023; **3**(30):259-290.

[24] Chow VT. **Hydraulics, Open-Channel, International Student Edition.** *McGraw-Hill*; 1954.

[25] Nash JE, Sutcliffe JV. **River Flow Forecasting through Conceptual Models Part I-A Discussion of Principles.** *Journal of Hydrology* 1970; **10**(3):282-290.

[26] Avila KC. **Evaluating Toe Erosion and Streambank Stability with BSTEM Model for Yonaba Creek.** *Research World International Conference*; 2016. ISBN: 978-981-925751-925753-925751.

[27] Mohammed-Ali W, Mendoza C, Holmes RR. **Riverbank Stability Assessment During Hydro-Peak Flow Events: The Lower Osage River Case (Missouri, USA).** *International Journal of River Basin Management* 2021; **19**(3):335-343.